Landscape Character Classification with a Deep Neural Network: A Case Study of the Jianghan Plain

Wenke Qin [1], Wenpeng Li [2], Zhuohao Zhang [2], Weiya Chen [2,3,4,*] and Min Wan [1,*]

1 School of Architecture and Urban Planning, Huazhong University of Science and Technology, Wuhan 430074, China; d202081123@hust.edu.cn
2 School of Civil and Hydraulic Engineering, Huazhong University of Science and Technology, Wuhan 430074, China; m202371912@hust.edu.cn (W.L.); d202480763@hust.edu.cn (Z.Z.)
3 National Center of Technology Innovation for Digital Construction, Huazhong University of Science & Technology, Wuhan 430074, China
4 International Joint Research Laboratory of Smart Construction, Wuhan 430074, China
* Correspondence: weiya_chen@hust.edu.cn (W.C.); minwan@hust.edu.cn (M.W.);
Tel.: +86-15902725652 (W.C.); +86-15827433777 (M.W.)

Abstract: Grounded in the theoretical and methodological frameworks of landscape character identification from the European Landscape Map (LANMAP) and landscape character assessment (LCA), this study developed an AI-based tool for landscape character analysis to classify the Jianghan Plain's landscape more effectively. The proposed method leveraged a deep learning model, the artificial intelligence-based landscape character (AI-LC) classifier, along with specific naming and coding rules for the unique landscape character of the Jianghan Plain. Experimental results showed a significant improvement in classification accuracy, reaching 89% and 86% compared to traditional methods. The classifier identified 10 macro-level and 18 meso-level landscape character types within the region, which were further categorized into four primary zones—a lake network river basin, a hillfront terrace, surrounding mountains, and a lake network island hill—based on natural and social features. These advancements contributed to the theoretical framework of landscape character assessment, offering practical insights for landscape planning and conservation while highlighting AI's transformative potential in environmental research and management.

Keywords: landscape character assessment; European landscape map; deep learning; Jianghan Plain

1. Introduction

Historically, landscape character classification has relied predominantly on professionals' expertise and subjective judgment. However, technological advancements have facilitated the emergence of more quantitative and objective classification methods in this field. Moreover, AI technology has introduced innovative concepts and methodologies into landscape architecture research. Using remote sensing images of the Jianghan Plain, this study applied the European landscape map (LANMAP) [1] method to classify landscapes on the basis of their natural characters. It further enhances this classification by implementing deep learning algorithms for refined landscape recognition, thus exploring new approaches and perspectives in landscape character classification research.

1.1. Background

In contemporary society, the decline and transformation of landscapes amidst the rapid currents of globalization and urbanization have attracted sustained global attention. Scholars have embarked on systematic investigations into the protection, planning, and management of landscapes. In 2002, the Rural Authority of England and Scottish Natural Heritage issued landscape character assessment (LCA) guidelines, which defined landscape quality as a landscape element that differentiates the landscape within a certain range,

rather than good or bad, and gives the site a unique feeling. Landscape character refers to the distinct and recognizable pattern of elements that consistently occur in a particular type of landscape. These elements include geology, landform, soils, vegetation, land use, field patterns, and human settlement, all of which combine to create a unique character, making each landscape distinct and providing its specific sense of place [2]. As an effective tool for analyzing landscape character, controlling landscape changes, and evaluating landscape value, LCA has been continuously studied and practiced worldwide. Most existing LCA studies have focused on the identification stage [3].

The results of landscape character recognition usually include landscape character in typology and landscape areas/units in chorology [4,5]. The identification methods of existing types and regions can be divided into two categories, namely digital and manual interpretation. Manual interpretations employ aerial images as the interpretation base and use heuristic methods to identify trait types and regions [6]. Furthermore, an integrated identification methodology combines both digital and manual approaches, offering a multi-faceted perspective [7]. Digital methods include clustering methods, overlay methods [8], and image segmentation [9]. Among them, clustering methods are the most commonly used, such as k-means clustering [10] and affinity propagation clustering [11]. Regarding the identification of landscape character, to express the change in scale from small to large, scholars usually use various terms to describe relative relationships, such as local, regional, national, micro/small/detail, meso/intermediate, and macro/large/general/broad, and this study employs a research approach that integrates meso-level and macro-level relationships [7]. For example, Li and Zhang [11] adopted a hierarchical identification in three scales, namely the broad scale for provincial zones, intermediate scale for cities, and detailed scale for towns.

In recent years, a growing consensus has emerged among scholars advocating for the integration of more rigorous quantitative methods in the examination of landscape character classification systems and indicators. For example, Wu et al. [12] employed a comprehensive methodology that integrated high-resolution imagery, drone technology, and extensive field surveys to investigate subtle distinctions in landscape character. They adopted a top-down approach for decomposition and classification to develop the landscape ecological classification (LEC) system within the MCSS (Mining Cities in the Semi-arid Steppe). Carlier et al. [13] implemented a series of clustering iterations for the objective multivariate classification of geomorphic landscape units and land cover datasets. Larrachea et al. [14] delineated central Argentina into two anthropogenic units and six natural landscape units, employing land use, the normalized difference vegetation index (NDVI), and other datasets for classification. Li et al. [15] developed a framework for the classification of complex agricultural landscapes with remote sensing data, utilizing iterative deep learning (IDL) techniques. Fang et al. [16] applied the k-means algorithm to overlay and categorize various landscape factors extracted from multispectral images, elevation data, and field survey information. Giang et al. [17] leveraged diverse socionatural profile data from satellites such as ALOS, NOAA, and multitemporal Landsat satellite imagery as inputs for a convolutional neural network (CvNet) model in coastal landscape character classification. Manual interpretation methods, while offering a high degree of reliability for researchers with substantial expertise, often demand a significant level of professional background and experience, making them less accessible for broader or non-specialist applications. In contrast, digital classification methods, such as k-means clustering, introduce a more objective framework; however, they carry the drawback of subjectivity in setting the number of clusters, which can impact classification accuracy and applicability in complex landscapes.

Currently, deep learning in landscape-related fields is increasingly centered on advancements in remote sensing and land use/land cover classification. This focus is driven by the growing body of research demonstrating how deep learning technologies enhance the analysis and interpretation of complex remote sensing data. By using remote sensing data, scholars have adeptly accomplished the extraction of building contours [18], the iden-

tification of urban functional zones [19], and the classification of various crops, farmlands, and greenhouses [20–23], as well as land cover classification [24]. Furthermore, within the realm of streetscape studies, scholars have analyzed urban streetscape architectural style [24], the green view rate [25], spatial perception [26–29], urban measurement [30], etc. Through the classification and identification of streetscape targets, one can evaluate urban street esthetic design and street walkability [31].

While previous research has extensively utilized clustering techniques and qualitative analyses to assess landscape character, the application of deep learning in remote sensing has been primarily concentrated on urban streetscapes, agricultural landscapes, and specific land use categories like farmlands and greenhouses. Such applications are rarely directed toward the classification of complex landscape characteristics, particularly within diverse and intricate environments.

Given the limitations of existing approaches, this study selects a highly varied landscape setting as a research subject, aiming to employ advanced intelligent analysis techniques. This approach not only addresses the challenge of classifying landscape characteristics in complex areas but also contributes to expanding the methodological scope of landscape research. The study underscores the need for innovative data-driven methodologies to improve the accuracy and applicability of landscape classification frameworks in diverse environments.

1.2. Research Objective

The principal objective of this research is to formulate a landscape character recognition model uniquely tailored for the Jianghan Plain that is capable of identifying various landscape characters at multiple scales within this region. The anticipated outcomes of this study are poised to become an indispensable tool for research and planning entities, facilitating a nuanced classification of landscape that transcends disciplinary boundaries. This paper delineated the selection of remote sensing data, elevation, land use, and soil classification as pivotal input variables to categorize landscapes of the Jianghan Plain, employing the LANMAP methodology. This study augmented the landscape character classification and recognition processes by using deep learning models and infusing them with sophisticated analytical capabilities. The study was further clarified by addressing the following research questions about landscape character classification of the Jianghan Plain:

1. What variety of landscape characters can be classified in the Jianghan Plain on the basis of natural and social characters via the LANMAP method and how should the corresponding scale for this classification be determined?
2. Is using deep learning models with remote sensing data a viable and efficient method for categorizing the landscape character of the Jianghan Plain?
3. What are the defining characters of macro–meso landscape character classification within the Jianghan Plain and how do these characters inform our understanding of the region's geography?

2. Materials and Methods

2.1. Study Area and Data

Drawing upon the natural landscape character classification structure of LANMAP in Europe [9], this study incorporated topography, climate environment, land use, and soil type as fundamental elements of the landscape character of the Jianghan Plain. Following the classification computation involving the overlay of multiple data layers, a comprehensive landscape character classification system was ultimately established for the region.

The Jianghan Plain, located in the south–central region of Hubei Province, China, spans approximately 46% of the province's total land area. It extends from Yichang City in the west to Huangmei City in the east and is bordered to the north by the Dabie, Tongbai, and Dahong Mountains, while its southern boundary reaches the Wuling and Mufu Mountains. The Yangtze River traverses the southern part of the plain from west to east, joined by its

largest tributary in the region, the Han River, which flows from northwest to southeast. This unique geographical setting, defined by a gradient that runs from west to east and north to south, also adjoins the Dongting Lake Plain in the central southern area. The research focus for this study is the area encompassed by the 50-meter contour lines along the Yangtze and Han River basins within Hubei Province [32,33].

As a microcosm of environmental interactions, the Jianghan Plain exemplifies the complex interplay between natural landscape and human activities, with a diverse topography and rich ecological habitats that provide a critical framework for landscape character classification [34]. Insights from this study, while rooted in the Jianghan Plain, offer valuable implications for environmental management and conservation, potentially informing landscape systems around the world. By examining the Jianghan Plain, this research not only enhances the local understanding of its distinctive environmental features but also contributes to broader sustainable landscape management practices, showcasing how regional studies can support large-scale environmental strategies.

To integrate the findings with current territorial spatial planning, the study's scope was extended to include the modern administrative regions within the boundaries above, encompassing nine provincial cities, 56 counties, and urban areas, collectively covering an approximate area of 84,908 km^2 (Figure 1).
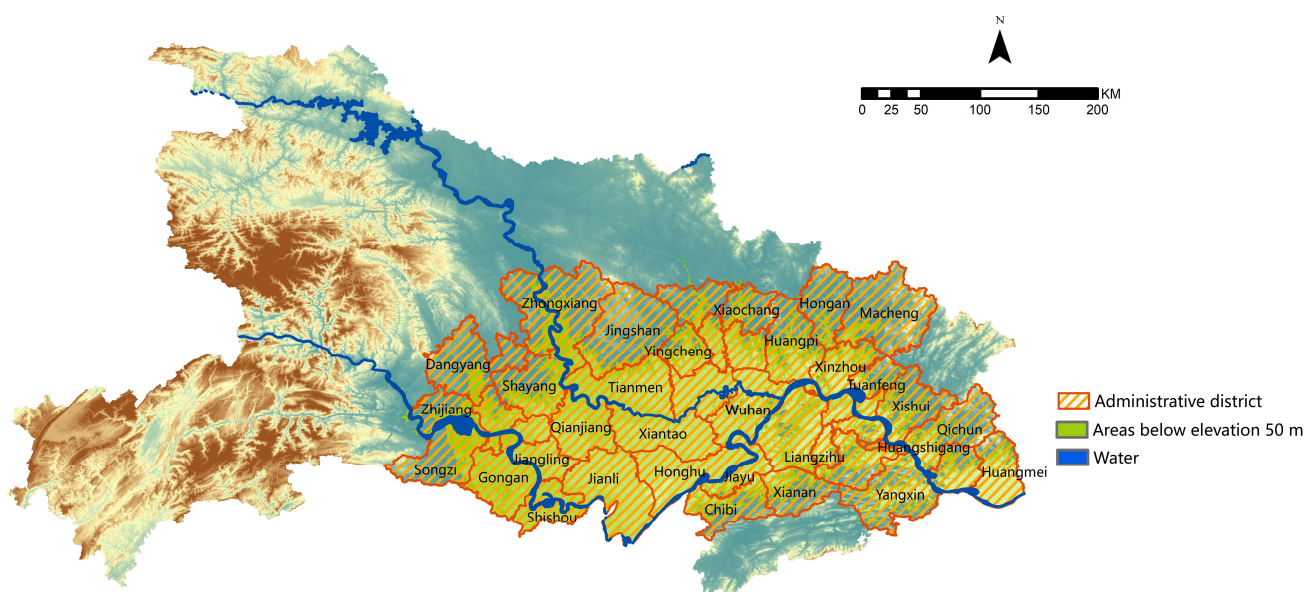

Figure 1. Map of the Jianghan Plain and its specific administrative boundaries.

The central and southern regions of the Jianghan Plain predominantly fall within the Jianghan fault prospecting zone of the Yangtze paragenetic platform. Here, vigorous sediment accumulation has resulted in the formation of a plain hinterland below 50 m above sea level. Owing to the unique amalgamation of land, water, heat, and soil, this area has transformed into a fertile region that is rich in fish and rice and marked by thriving human settlements [35]. The following section provides a summary of the region's topography, climate, soil type, land use, and other pertinent natural background conditions.

The Jianghan Plain hinterland is surrounded by mountain ranges on three sides and intersects with the major tributaries of the Yangtze River and Han River. This region is abundant in lakes, wetlands, rivers, and canals. Climatically, the Jianghan Plain is characterized by a northern subtropical humid monsoon continental climate, with concurrent rainfall and warmth in the same season and four distinct seasons. Over 70% of its annual precipitation occurs in the spring and summer, with the river's flood season frequently experiencing heavy rains and rainstorms, posing significant risks of flooding and soil erosion. With approximately 2000 h of sunshine annually, the region boasts abundant light and heat

resources, creating favorable conditions for crop cultivation. In terms of soil composition, the Jianghan Plain predominantly consists of river alluvium and lake sediments, with thick sandy loam primarily situated along the two rivers. As one moves farther from the rivers, the clay content of the soil increases, resulting in the formation of more viscous lacustrine soil in low-lying lakes. This advantageous regional environment nurtures ideal land for fish and rice. Regarding land use, the Jianghan Plain predominantly features cultivated land interspersed with water bodies and the surrounding hills graced with woodlands.

2.2. Method

Within the machine learning module for landscape character classification and recognition (Figure 2), via a series of iterative experiments, various sizes of landscape character research units were established, and remote sensing data were segmented according to these unit scales to create a unified dataset. The landscape character classifications derived from the previous module were employed to annotate the dataset according to their geographical locations. Notably, the dataset was annotated with varying numbers of landscape characters depending on the scale of analysis. However, initial analyses of the annotated dataset revealed that the direct application of LANMAP-based landscape characters for learning led to suboptimal results. This issue arises because specific landscape characters, classified by natural–social features and meeting the area threshold criteria for landscape recognition, exhibit similar visual characters. Consequently, a category optimization module was utilized to amalgamate landscape characters with similar characteristics, aiming to enhance the outcomes in subsequent learning phases.

Figure 2a provides an overview of the workflow, organized into two core components, the landscape character classification module and the machine learning module.
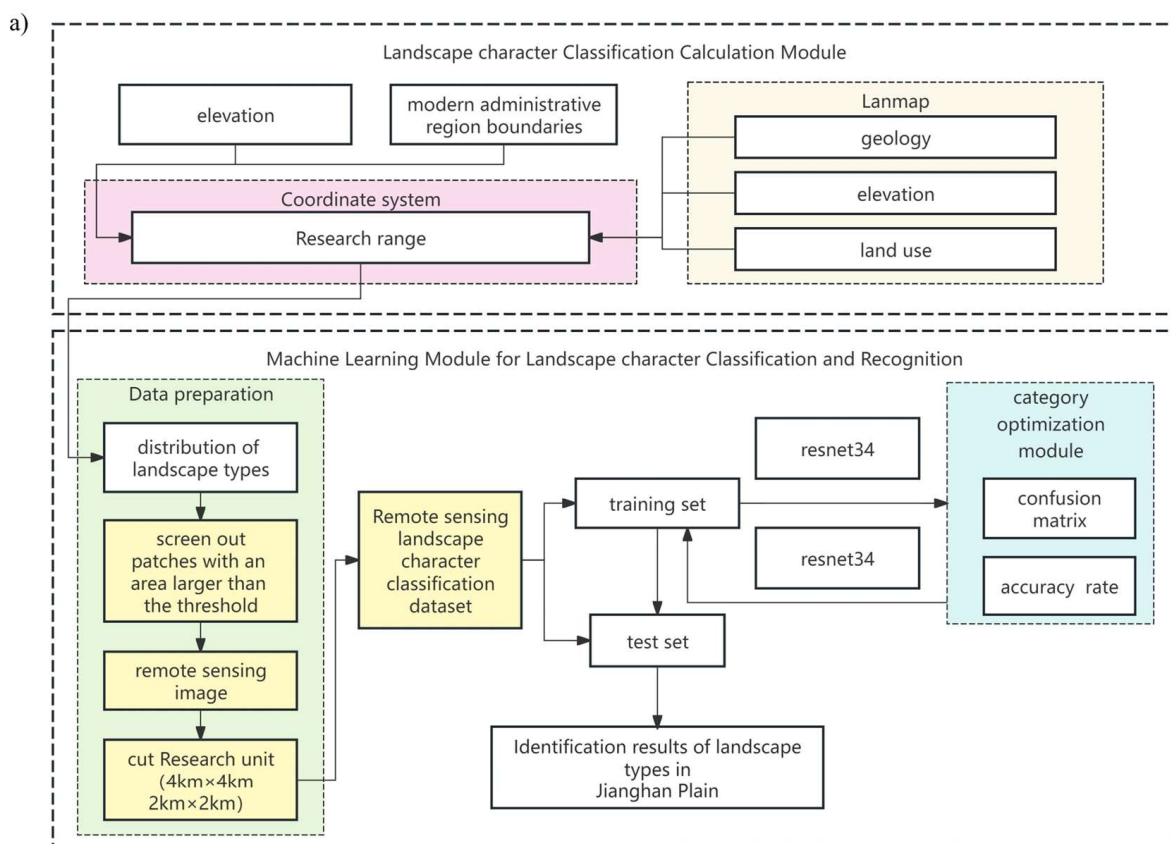

Figure 2. *Cont*.
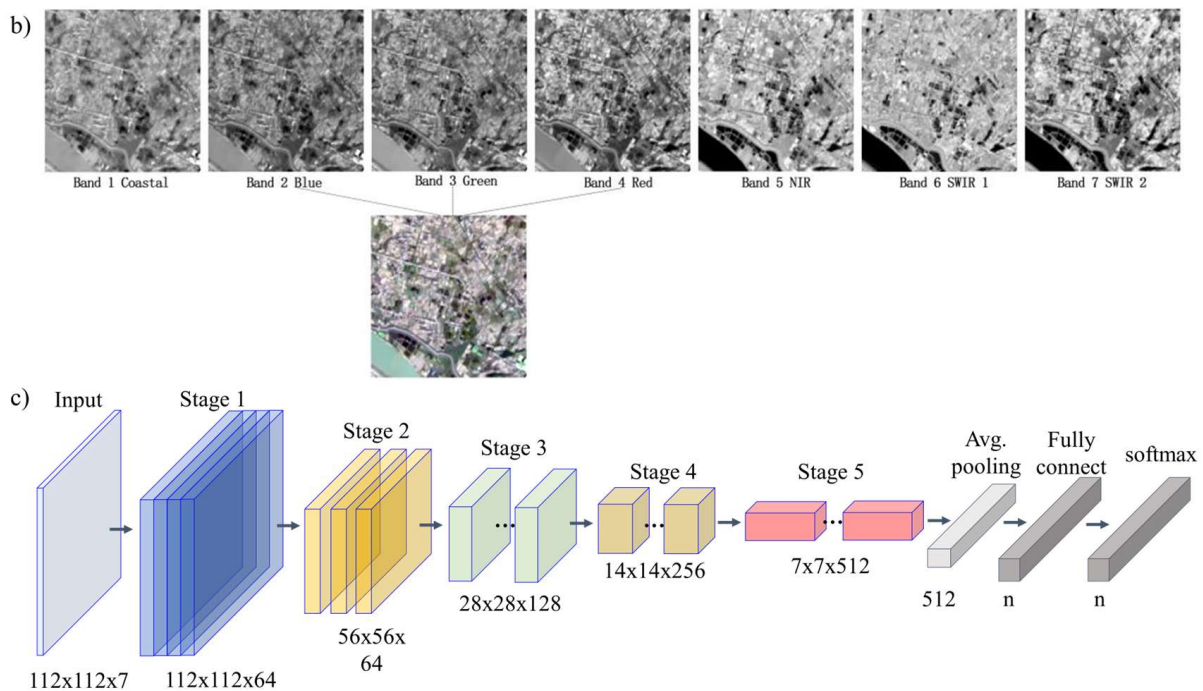
Figure 2. Description of system architecture. (**a**) Landscape character classification and recognition system; (**b**) remote sensing images of different channels; (**c**) convolutional neural network model used in classification system.

Landscape character classification module (Figure 2a, left): This module employed administrative boundaries, the study area extent, Landsat geocoding, elevation, and land use data to establish an accurate coordinate framework and assemble the landscape dataset. Primary tasks involve mapping landscape character type distributions, filtering regions meeting a minimum size threshold, sourcing remote sensing images, and segmenting research units at 4 km × 4 km and 2 km × 2 km spatial scales.

Machine learning module (Figure 2a, right): With the dataset prepared, a ResNet34 deep residual network (architecture shown in Figure 2c) was trained to classify landscape character types. Remote sensing images were divided into training and testing sets, with model performance evaluated via confusion matrices and accuracy metrics. Initial analyses showed that combining visually similar landscape characters in this module improved classification accuracy.

2.2.1. Landscape Character Coding

Drawing upon the findings of the European LANMAP eco-physical method [1], this study suggests that the perceptible characters of landscape are predominantly influenced by climate, topography, and geology. Moreover, cultural and socioeconomic factors are crucial in shaping land use patterns. Given that the Jianghan Plain is within a consistent climate zone, this study utilized three datasets stored in three layers—elevation, geology, and land use—as the foundational data for landscape character classification and identification.

Prior to data processing, a naming convention was established to delineate the type of landscape character classification, which was achieved by overlaying data from three layers, namely soil, elevation, and land use. In this study, geological data were classified into the following five categories, informed by classifications in previous studies and the current study's requirements: (1) paddy and swamp soil; (2) tidal sand soil; (3) red soil; (4) yellow, yellow-brown, and brown soil; and (5) lime and purple soil. The terrain data were segmented into seven categories according to elevation as follows: 0–30 plain; 30–50, low downland; 50–70, downland; 70–200, hill; 200–500, low mountain; 500–1000, middle mountain; and more than 1000, mountain. The land use classification adhered to the nine

categories presented in the original data, which were farmland, forest, shrub, grassland, water, ice, bare land, city, and wetland.

These categorical data served as the inputs for segmenting landscape characters, which were superimposed via the *Intersect* function in ArcGIS v10.8, thereby segmenting the target area into patches of varying sizes. Using the established naming rule, which integrates patch attribute characters, all patches were systematically recorded in the format of x-x-x (elevation–soil category–land use category) (Figure 3). Theoretically, when the naming rule is applied on the basis of elevation, soil quality, and land use, one could identify up to 315 ($5 \times 7 \times 9$) distinct landscape characters. However, in reality, only 110 of these combinations exist in the Jianghan Plain. Given that this research focused on macro-/meso-scale landscape character analysis, it was necessary to simplify the land types and select a limited number of landscape characters by establishing a threshold. An analysis of the curves correlating to a landscape character with patch areas indicated that at a threshold of 1000 km^2, the diversity of landscape characters tended to stabilize. In contrast, at a threshold of 100 square kilometers, there was a rapid decrease in diversity (Figure 3). Consequently, the study established 1000 km^2 and 100 km^2 as area thresholds for macro- and meso-landscape characters on the Jianghan Plain. This approach enabled the exclusion of patches exceeding these thresholds and the amalgamation of smaller patches into larger ones on the basis of the most extended neighboring intersecting lines (utilizing the *elimination* function in ArcGIS), resulting in the identification of 15 macro and 41 meso-landscape characters (Table 1, x-x-x means (elevation–soil category–land use category), Figure 4. For example, 1-1-1 means (0–30 plain–paddy soil, swamp soil–farmland)).
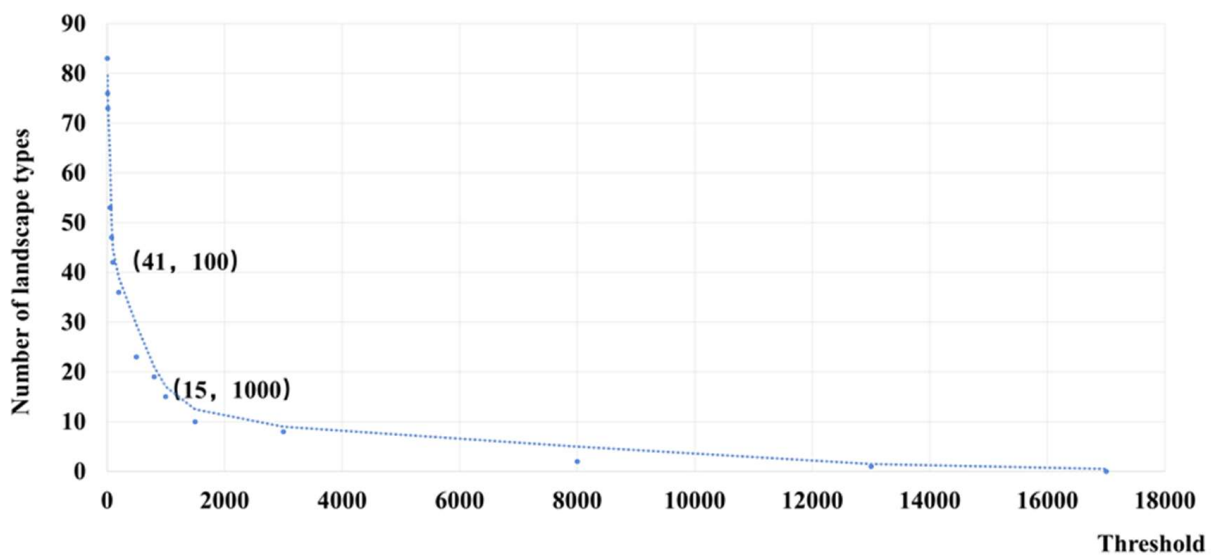

Figure 3. Distribution of landscape character area thresholds in the Jianghan Plain.

Table 1. Landscape character with area larger than the threshold.

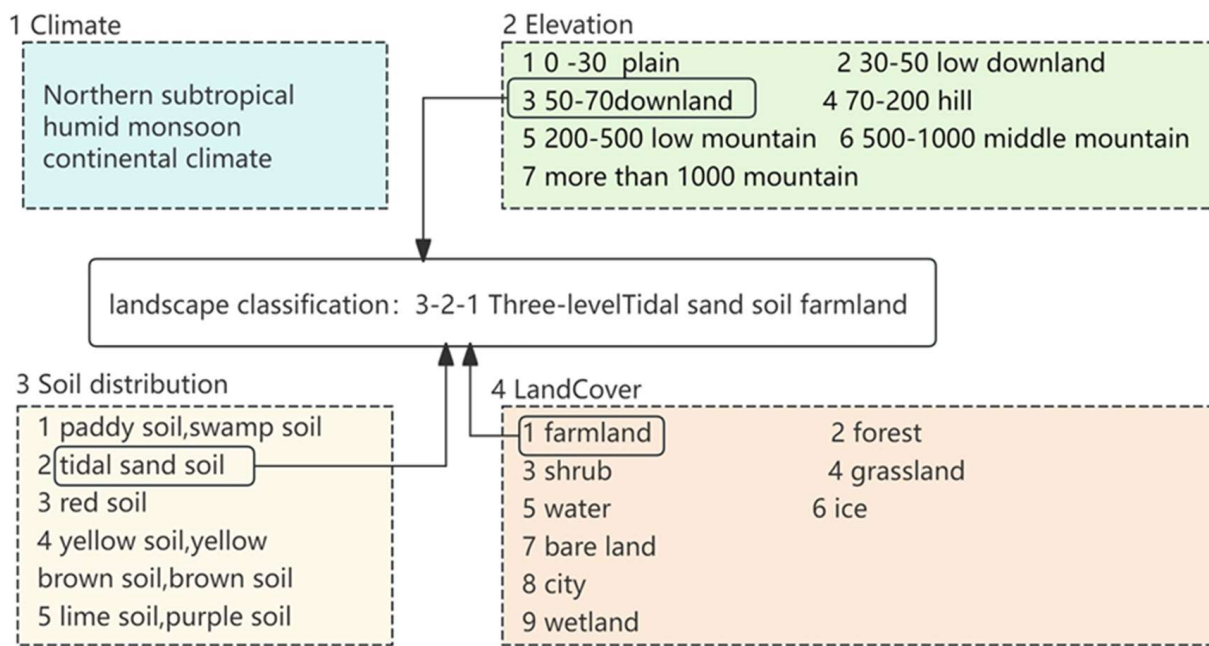| Threshold	Quantity of Types	Landscape Character Coding
1000 km^2	15	1-1-1, 1-1-5, 1-1-8, 1-3-1, 1-3-5, 2-1-1, 2-3-1, 2-4-1, 3-1-1, 3-4-1, 4-3-2, 4-4-1, 4-4-2, 4-5-1, 5-4-2
100 km^2	41	1-1-1, 1-1-5, 1-1-8, 1-2-1, 1-3-1, 1-3-5, 1-3-8, 1-4-1, 2-1-1, 2-1-5, 2-1-8, 2-2-1, 2-3-1, 2-3-2, 2-3-8, 2-4-1, 2-5-1, 3-1-1, 3-2-1, 3-3-1, 3-3-2, 3-4-1, 3-4-5, 3-4-8, 3-5-1, 4-1-1, 4-2-1, 4-3-1, 4-3-2, 4-4-1, 4-4-2, 4-4-5, 4-4-8, 4-5-1, 4-5-2, 5-3-2, 5-4-1, 5-4-2, 5-5-2, 6-3-2, 6-4-2

Figure 4. Naming and coding rules of landscape characters for Jianghan Plain.

2.2.2. Machine Learning Module

This study employed remote sensing imagery as the primary data source and applied transfer learning with the ResNet34 model [36], leveraging its pre-trained features to enhance landscape character classification. The input imagery consisted of Landsat 8 OLI multispectral satellite images with a spatial resolution of 30 meters, captured on 26 August 2020 under clear conditions with less than 10% cloud cover. These bands provided three color (RGB) channels and four infrared channels, resulting in a comprehensive seven-channel dataset. The remote sensing imagery was then superimposed with the landscape character classification map, enabling landscape character type annotations on the images based on locational correspondence. This approach derived the essential landscape character classification data, as illustrated in Figure 5.

Following extensive experiments, this study established 4 km × 4 km and 2 km × 2 km as the dimensions for the macro- and meso-landscape research units, respectively. A small area encompassing all landscape characters was selected from the center of the complete remote sensing image. The small area with a shape of (7531, 7691) pixels was subdivided into 4 km × 4 km and 2 km × 2 km patches. The dataset was expanded by shifting this segment by 1 km and 0.5 km each time, resulting in 9732 and 77,598 input images for macro- and meso-scale research, respectively (Table 2). Subsequently, the correlation between the remote sensing image and landscape character, as established in the previous step, was used to annotate each landscape research unit, thereby finalizing the data annotation process (Figure 6). When multiple landscape characters were present within a single study unit, the type with the largest area proportion was designated as the label. In the third step, each square was augmented and transformed into an input format comprising seven channels with a resolution of 112 × 112 pixels. During the experiment, images of various scales were divided into two groups, with 80% of the data allocated for training and 20% allocated for testing.
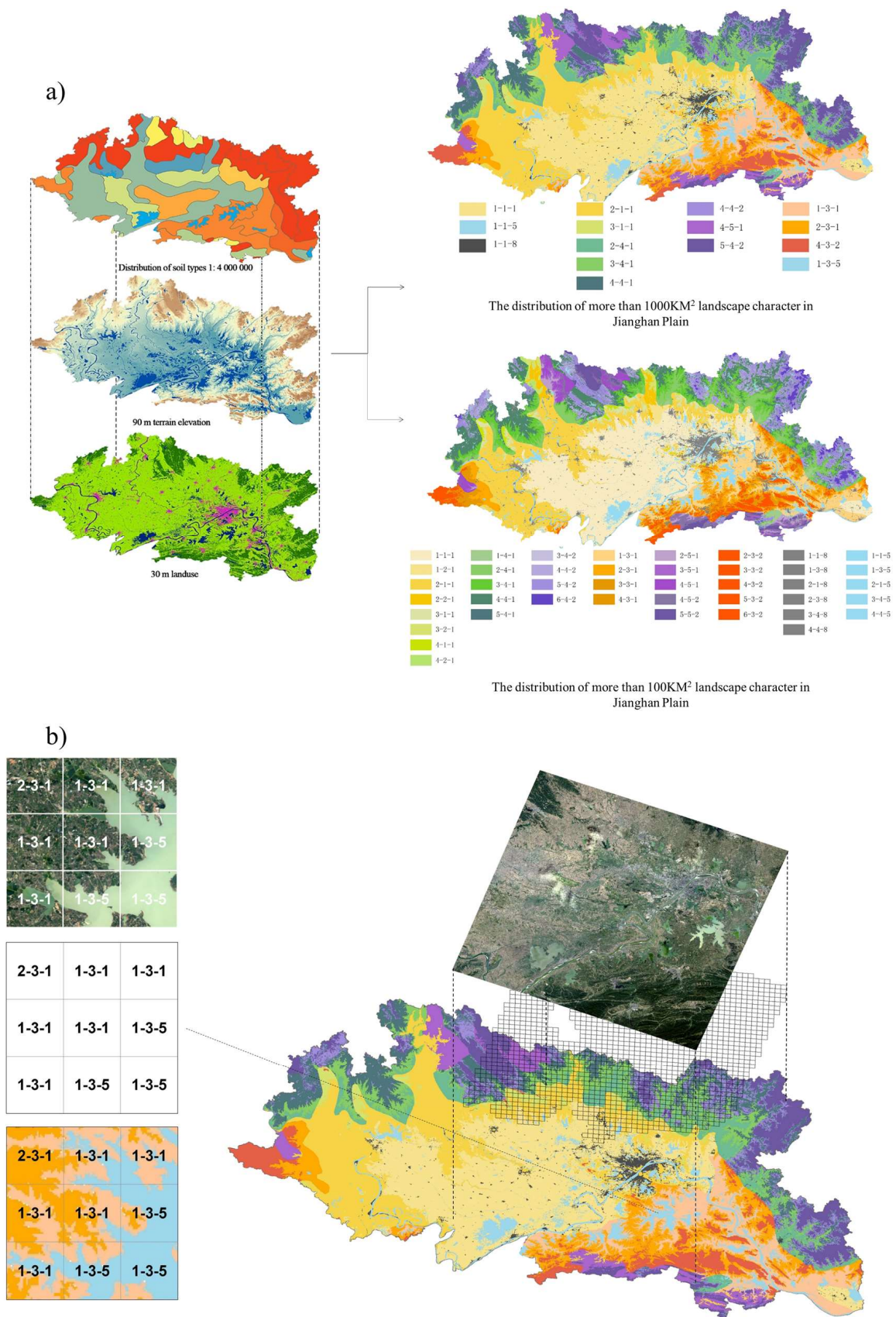
Figure 5. Maps showing (**a**) a landscape character distribution map of the Jianghan Plain. (**b**) Landscape character labeling process for the Jianghan Plain.

Table 2. Description of the Jianghan Plain landscape character dataset.

	Threshold	Number of Landscape Characters	Unit Area	Number of Slices	Number of Samples in the Training Set	Number of Samples in the Test Set
Macro	1000 km^2	15	4 km × 4 km	9732	7785	1947
Meso	100 km^2	41	2 km × 2 km	77,598	62,078	15,520

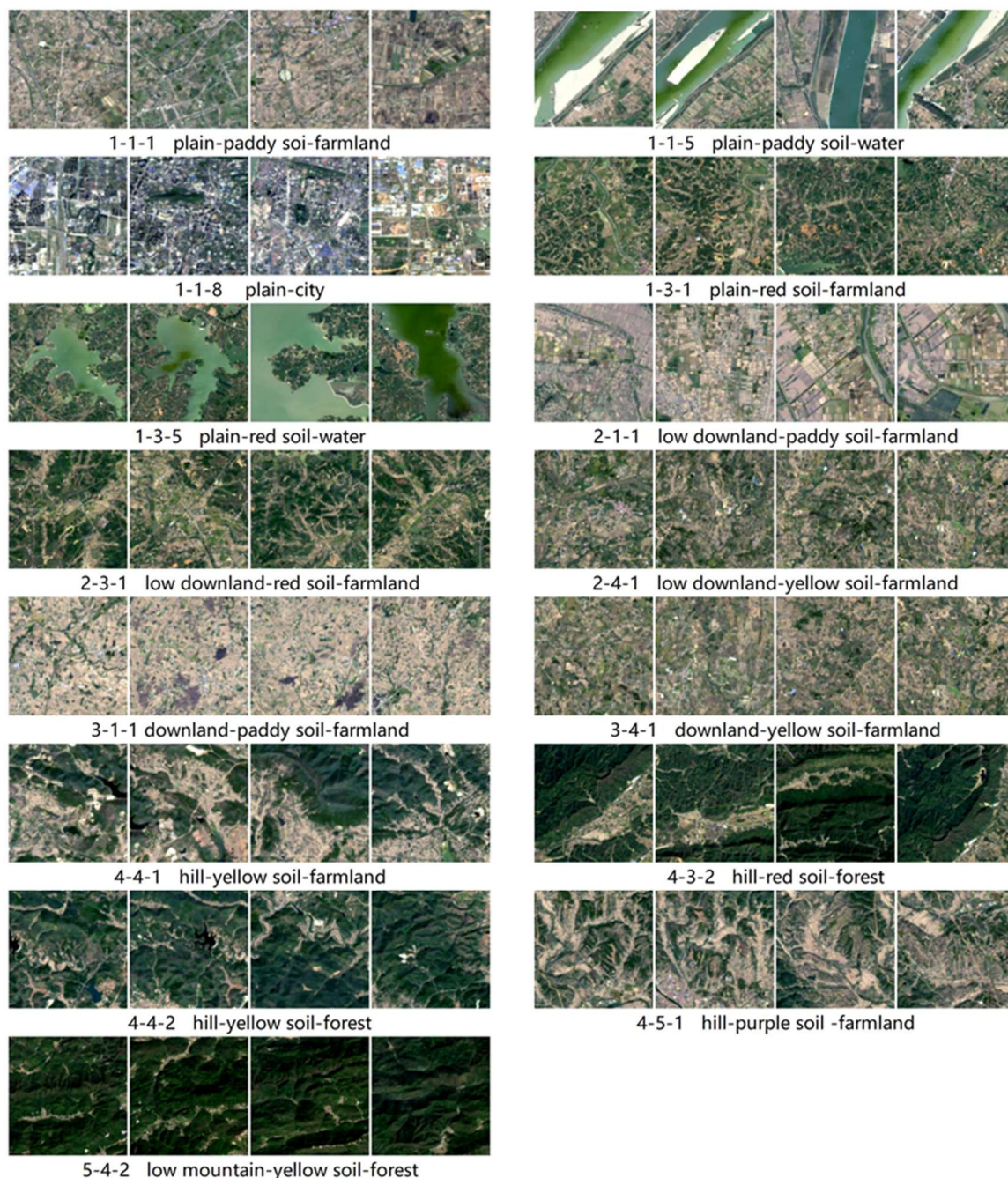Figure 6. Landscape character classification of the 4 km × 4 km area.

Convolutional neural networks (CNNs) are powerful feed-forward neural networks with multilayer convolutional structures that capture local image patterns effectively by addressing translation, rotation, and scaling issues, thus enhancing robustness [37]. As network depth increases, models gain more abstract feature representations, but deep layers

can introduce gradient problems. Residual networks (ResNets) mitigate this problem by learning "residual" functions through shortcut connections, allowing information to bypass certain layers and prevent gradient vanishing [36]. In this study, ResNet-34 processed multispectral remote sensing images, combining RGB and four infrared channels into seven-channel composite images. The model's input was normalized to $112 \times 112 \times 7$ dimensions to accommodate these data.

Considering the complexity and volume of data involved in landscape character classification, the ResNet-34 model was chosen as the backbone for this task. Modifications to the original ResNet-34 network were implemented to accommodate input images of varying sizes. Given that the original ResNet-34 network was designed for input image resolutions of $224 \times 224 \times 3$, which differs from our data resolution, the convolution kernel size of the network's first convolutional layer was altered from $7 \times 7 \times 3$ to $7 \times 7 \times 7$, and the stride parameter was set to 2. Consequently, this adjustment resulted in an input size for this layer of $112 \times 112 \times 7$ and an output size of $112 \times 112 \times 64$, aligning with the output size of the original network's first convolutional layer. During the training phase, the final fully connected layer parameters were configured on the basis of the number of categories identified in the landscape character classification task. For landscape character classification tasks at the macro-, meso-, and micro-scales, the number of neurons in the last fully connected layer was set to 15, 44, and 80, respectively. The network parameters used for landscape character classification tasks are delineated in Table 3.

Table 3. Parameter settings of the ResNet34 network.

Layer Name	Output Size	Input Size	Macro-Scopic	Meso-Scopic	Micro-Scopic
Conv1	$112 \times 112 \times 64$	$112 \times 112 \times 7$		7×7, 64, stride 2	
Conv2_1 ~ Conv2_3	$56 \times 56 \times 64$	$56 \times 56 \times 64$		3×3, 64 3×3, 64	
Conv3_1	$28 \times 28 \times 128$	$56 \times 56 \times 64$		3×3128, stride 2 3×3128	
Conv3_2 ~ Conv3_4	$28 \times 28 \times 128$	$28 \times 28 \times 128$		3×3128 3×3128	
Conv4_1	$14 \times 14 \times 256$	$28 \times 28 \times 128$		3×3, 256, stride 2 3×3256	
Conv4_2 ~ Conv4_6	$14 \times 14 \times 256$	$14 \times 14 \times 256$		3×3256 3×3256	
Conv5_1	$7 \times 7 \times 512$	$14 \times 14 \times 256$		3×3512, stride 2 3×3512	
Conv5_1 ~ Conv5_3	$7 \times 7 \times 512$	$7 \times 7 \times 512$		3×3512 3×3512	
Classifier	$1 \times 1 \times 512$ $1 \times 1 \times 15/44/80$	$7 \times 7 \times 512$ $1 \times 1 \times 512$	FC-15	Average pool FC-44	FC-80

For each landscape character classification task undertaken, a consistent set of hyperparameters was employed during training. The stochastic gradient descent (SGD) optimizer was employed with a mini batch size set to 4. The learning rate was 0.01 and the models underwent training for up to 300 epochs. During the data pre-processing phase, various data augmentation techniques, including random horizontal flipping, vertical flipping, and rotation, were applied.

After model training was completed, a comprehensive evaluation was conducted to ascertain the model's predictive accuracy and generalizability. This assessment was conducted in two stages, the classification accuracy was the primary index for assessing model performance, and the confusion matrix was further analyzed to fuse visually similar classes [38]. Accuracy reflects the proportion of samples correctly classified by the model, which is calculated as the sum of true positives (TPs) and true negatives (TNs) divided by the total number of samples. The confusion matrix offers a more detailed view of the model's performance across different categories, including true positives, false positives

(FPs), true negatives, and false negatives (FNs). The confusion matrix revealed that certain misclassified landscape character types, despite having distinct features such as soil types and elevation, are indeed very similar to each other in visual channels.

To address this challenge, a category optimization module was introduced. This module uses a confusion matrix optimization approach, where each element in the matrix is analyzed to determine which category pairs should be merged. For each pair of categories i and j in the confusion matrix, their combined score S was calculated as

$$S(i, j) = M[i, j] + M[j, i] \tag{1}$$

In this context, M denotes the confusion matrix, where M[i, j] represents the number of instances where class i was erroneously classified as class j, and M[j, i] indicates the instances of class j being misclassified as class i. Subsequently, the pair of categories with the highest score, S, was selected for merging, with the argmax function determining the optimal category pair (i, j) that maximizes S.

$$(i*, j*) = \arg \max(i, j)S(i, j) \tag{2}$$

After merging, the selected category pairs were consolidated and eliminated from the category list. The confusion matrix was revised, integrating the rows and columns corresponding to the merged categories. This merging procedure was executed iteratively, adhering to a predefined maximum number of merges and retrograde iterations. Following each iteration, a new classification report was produced to evaluate any changes in performance. Upon acquiring the revised classification, the data were resubmitted for model training to enhance the overall performance.

3. Results

3.1. Research Scale Analysis

With respect to landscape character classification, we identified 15 and 41 distinct landscape character types at the macro- and meso-scales, respectively (Figure 3). Following the optimization of landscape character, the number was reduced to 10 and 18 for the macro- and meso-scales, respectively.

At the macro-scale, the landscape predominantly consisted of farmlands on plains, watershed cities, highlands, low hills, and hills, as well as woodlands in hilly lowland zones. At this scale, the hinterland of the plains was characterized by an abundance of farmland, water, and urban landscapes, with an increasing proportion of woodlands correlated with an increase in elevation, thus altering the landscape character. Moreover, in the southeastern region of the Jianghan Plain, the intermingling of the two rivers at their confluence and the numerous water areas resembling tree branches with hilly terrain culminated in unique landscape formations. At the meso-scale, the reduced scale led to a refined delineation of landscape character, encompassing varied farmland and urban areas at different altitudes, woodlands in the highland and mesas, and water bodies in the terrain transition zones. This observation underscores the importance of defining the scale of the study area in landscape character research.

The optimization results revealed distinguishable landscape character, such as low-elevation farmland in the central Jianghan Plain (1-1-1), the paddy soil and yellow soil farmland transitioning from the northern Tongbai Mountains and the southern foothills of the Dabie Mountains to the plains (2-1-1, 3-1-1, etc.), and the red soil farmland transitioning from the southeastern Mugao Mountain to the plain area (2-3-1, 1-3-1). After optimization, these types still belong to different categories. However, a higher similarity between paddy soil and yellow soil farmland was observed when transitioning northward from the central plain into the low downland, downland, and hill areas (2-1-1, 3-1-1, 2-4-1, 3-4-1, 4-4-1). During optimization, these types were merged.

3.2. Performance Evaluation

The experimental data presented in Table 4 indicate that the accuracies achieved by learning the landscape character directly from the landscape character classification calculation module were 82% and 78%, respectively. Some examples of classification results are shown in Figure 7. Following the application of the category optimization module, this rate could be increased to 89% and 86%, respectively. Furthermore, the experimental results corroborate the stability and accuracy of the model in the intelligent recognition of landscape character classification.

Table 4. Experimental results of the landscape character classification model.

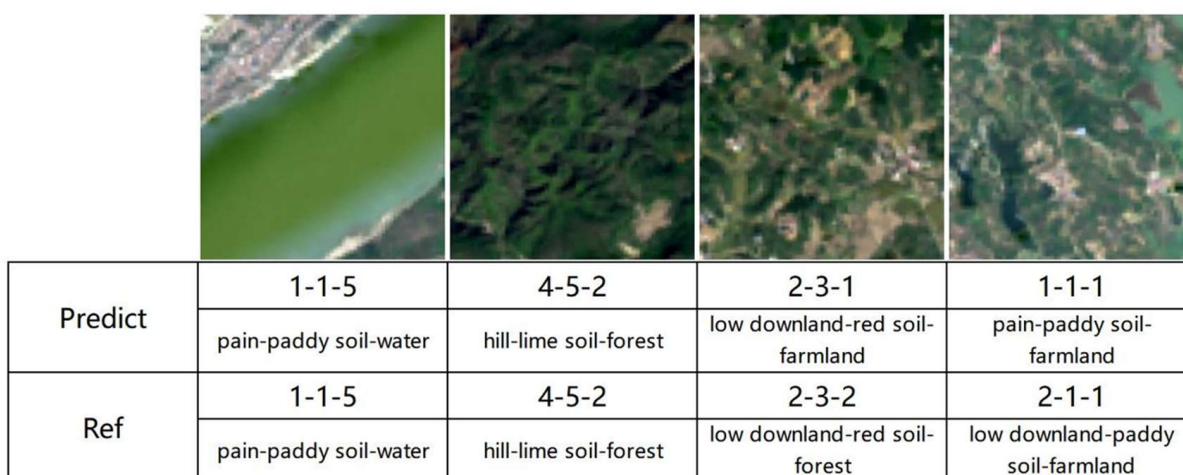|	Unit Area	Number of Types Before Optimization	Average Accuracy Before Optimization	Number of Types After Optimization	Average Accuracy After Optimization
Macro	4 km × 4 km	15	0.82	10	0.89
Meso	2 km × 2 km	41	0.78	18	0.86

Figure 7. Examples of right and wrong classification results.

4. Discussion

4.1. Assessment of the Effectiveness of the AI-LC Classifier

This study culminated in the development of a multiscale landscape character classification system encompassing two distinct levels, namely macro-scale and meso-scale levels. Historically, landscape character classifications have been predominantly determined by professional experts without quantitative indicators, relying solely on landscape indices, which are insufficient for fully representing the social attributes of landscapes. The current landscape character classification, which is based on elevation, land use, and soil, offers a more comprehensive understanding of the determinants of plain landscapes. By utilizing the AI landscape character classification and recognition model, this research achieved intelligent landscape character classification and recognition, incorporating both natural and social attributes. This research methodology is notably expandable, and the well-trained ResNet34 model holds significant value for national and global landscape character research. Unlike traditional landscape character classification methods that rely on expert experience, this approach requires scientists to (1) calculate landscape character classification via LANMAP at various research scales, (2) segment remote sensing images according to these scales and annotate them with classifications from Step (1) to compile the dataset, (3) input this dataset into the learning model, and (4) execute the model and optimize for subsequent relearning.

In this study, the 15 data types underwent further classification, resulting in the macroscopic landscape of the Jianghan Plain being segmented into four primary categories, a lake network river basin, lake network island hills, pre-mountain platforms, and a hillfront terrace (Table 5). Each category within the macroscopic landscape of the Jianghan Plain features distinct meso-level landscape character codes and grouping principles based on factors such as topography, elevation, and soil type. For instance, the lake network river basin category is primarily located in the central areas of the Jianghan Plain, characterized by low elevation and an intricate network of waterways. The lake network island hills category, on the other hand, is situated in the southern region of the plain, defined by a mosaic of lake networks and island-like hills. Additionally, the pre-mountain platforms and hillfront terrace categories are located on the periphery of the Jianghan Plain, each marked by distinct features; the pre-mountain platforms are associated with higher mountain elevations, while the hillfront terrace areas are identified by elevated terrain transitioning to the foothills.

Table 5. Macroscopic landscape division of the Jianghan Plain.

Macro-Landscape Character Coding	Meso-Landscape Character Coding	Grouping Principles	Location	Types
1-1-5 1-1-1 1-1-8	1-1-1 1-1-5 1-1-8	Low-Altitude Farmland with Alluvial and Paddy Soils	Heartland of the Jianghan Plain, characterized by flat terrain and a crisscrossing network of waterways	Lake and River Basins
4-5-1 4-4-2 5-4-2	4-4-2 5-4-2 6-4-2 **3-4-5 4-4-5** 2-5-1 3-5-1 4-5-1 4-5-2 5-5-2 **3-4-8** **4-4-8** 4-1-1 4-2-1	High-Altitude Outer Ring Mountain Forests	Outer ring mountains of Jing, Dahong, Tongbai, and Dabie ranges surrounding the Jianghan Plain	Surrounding Hill Ranges
1-3-1 2-3-1 1-3-5 4-3-2	1-3-1 2-3-1 3-3-1 4-3-1 2-3-2 3-3-2 4-3-2 5-3-2 6-3-2 1-3-5 **1-3-8 2-3-8**	Intermingled Mid- and Low-Altitude Red Soil Farmland	Lake network island hills, south of the confluence of two rivers on the Jianghan Plain	Lake Network Island Hills
2-1-1 3-1-1 2-4-1 3-4-1 4-4-1	1-2-1 2-1-1 2-2-1 3-1-1 3-2-1 1-4-1 2-4-1 3-4-1 4-4-1 5-4-1 2-1-5 **2-1-8**	Mid- to High-Altitude Yellow-Brown Soil Farmland	Hillfront terrace, convergence area of Jing, Dahong, Tongbai, and Dabie Mountains with the Jianghan Plain	Hillfront Terrace

These four unique landscape categories encapsulate the distinct natural characteristics inherent to various regions of the Jianghan Plain. Specifically, the lake network and river basin area, characterized by the least undulation and lowest elevation within the Jianghan Plain, boasts a broad flat terrain, an intricate network of waterways, the most significant proportion of arable land, and a minor proportion of forested areas (1-1-1, 1-1-5, 1-1-8). The landscape in this region is significantly influenced by the collective impact of lakes, water systems, and ditches, leading to the emergence of varied farmland patterns such as dykes, grids, and curved networks [39].

The hillfront terrace area is a transitional zone from the hinterland plains to the low hills, characterized by a more pronounced undulation and elevation than the lake network and river basin areas. This area boasts a high proportion of arable land, predominantly terrace fields (2-1-1, 3-1-1, etc.). Additionally, forested land, indicative of the hill landscape, has expanded, with pre-hill lakes situated at the interface of the hill and plain.

The lake network island hill area exhibits elevation and undulation levels between the lake network river basin and the hillfront terrace, with its forest and farmland intertwining with each other (1-3-1, 2-3-1, 4-3-2) and its water area being the most extensive among the four categories (1-3-5). The region features island-like hills interspersed with tree fork-shaped lakes, where the Yangtze and Han rivers converge, thereby crafting the unique landscape characteristics of this area [40].

Surrounding the mountains, the hills are the highest in elevation with steep terrain slopes, leading to a limited area of arable land and a predominant presence of forested land in this region (4-4-2, 5-4-2). The region is further characterized by river valleys, valley plains, and scattered reservoirs, serving as hallmark features of this landscape (3-4-5, 4-4-5).

4.2. In-Depth Analysis of Landscape Classification Results

Unlike previous studies that mainly focused on identifying specific objects in remote sensing image data [18,19], this paper achieves a direct recognition and classification of landscape character types to which remote sensing images belong. Using the AI-LC classifier, this study not only facilitates the classification and recognition of landscape character types but also, through the process of category optimization, provides novel insights into the interrelationships among landscape character type characteristics. From a macro-perspective, the system initially categorized the Jianghan Plain into 15 major categories. Leveraging AI recognition capabilities, the 15 initially identified categories were further optimized to 10, increasing the accuracy rate to 89%. The optimization results revealed distinguishable landscape characters, such as low-elevation farmland on the central Jianghan Plain (1-1-1), paddy soil and yellow soil farmland transitioning from the northern Tongbai Mountains and the southern foothills of the Dabie Mountains to the plains (2-1-1, 3-1-1, etc.), and red soil farmland transitioning from southeastern Mugao Mountain to the plain area (2-3-1 and 1-3-1). However, a greater similarity between paddy soil and yellow soil farmland was observed when transitioning northwards from the central plain into the low downland, downland, and hill areas (2-1-1, 3-1-1, 2-4-1, 3-4-1, and 4-4-1). Consequently, the landscape characters of the northern low-elevation farmland exhibit notable changes compared with those of the central low-elevation farmland primarily due to the varying terrain relief. Moreover, southern low-elevation farmland, characterized by numerous distinct water bodies, has undergone significant alterations in its landscape character (Figure 8a).

From the mesoscopic perspective, following the reduction in the threshold area, the number of landscape character types expanded from an initial 10 to 18 after category optimization (Table 4). The lowering of the landscape character type area threshold and the decrease in the size of the identification unit clearly led to the emergence of additional new landscape characters. For example, landscape characters 3-4-5 and 4-4-5 (height yellow loamy waters and hill yellow loamy waters, respectively) emerged, which are indicative of the landscape attributes of mountainous reservoirs in the Jianghan Plain (Figure 8b). This observation is consistent with the landscape character in which lakes are prone to form in areas experiencing significant topographic slope changes, especially where multiple rivers from the outer ring of the mountains converge onto the Jianghan Plain [41]. Moreover, the emergence of landscape characters such as 1-3-8, 2-1-8, 2-3-8, 3-4-8, and 4-4-8 (Table 5) reflects the inclusion of more urban towns as the study scale narrowed, indicating that this meso-scale study extended into the domain of habitat analysis (Figure 8c). These variations in habitat identification underscore the diversity in habitat characters across different locations in the Jianghan Plain, presenting a direction for future research endeavors

However, a reduction in research scale does not invariably lead to an increased landscape character type; in some instances, it may also decrease. As the scale decreases to a certain extent, different landscape characters may exhibit more remarkable similarities to one another. For example, in the case of the two water-type landscapes, i.e., 1-3-5 and 1-1-5, the distinction in their features at the 4 km × 4 km scale was more pronounced than that at the 2 km × 2 km scale, owing to the inclusion of more surrounding environmental factors. A parallel scenario was observed in the 5-4-2 and 4-4-2 woodland landscapes, where the decrease in patch size led to a loss of distinct features, thereby increasing the similarity between these landscapes (Figure 9).

At the mesoscopic research scale, the present resolution of remote sensing images may be low, raising questions about whether enhancing this resolution could improve the accuracy of recognition outcomes and support subsequent higher-precision research

endeavors. This consideration forms a pivotal direction for future research. As the research scale varies, the proliferation of landscape characters and the reduction in their coexistence suggest that different scales may be required for various landscape characters. This notion introduces a challenge that necessitates future research.
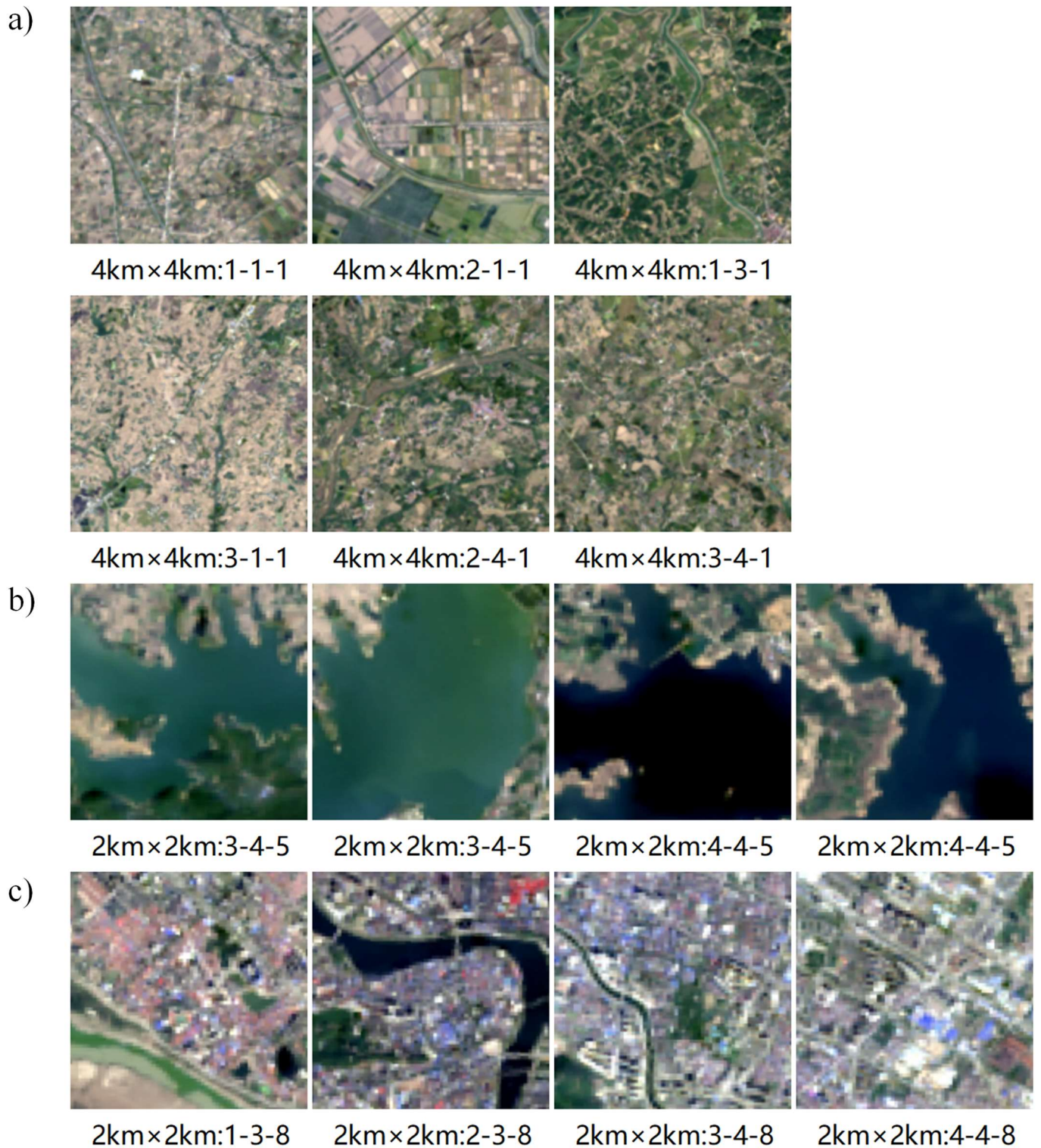

Figure 8. Maps showing (**a**) low-elevation farmland of 4 km × 4 km unit. (**b**) New added water landscapes of 2 km × 2 km unit. (**c**) New added city landscapes of 2 km × 2 km unit.
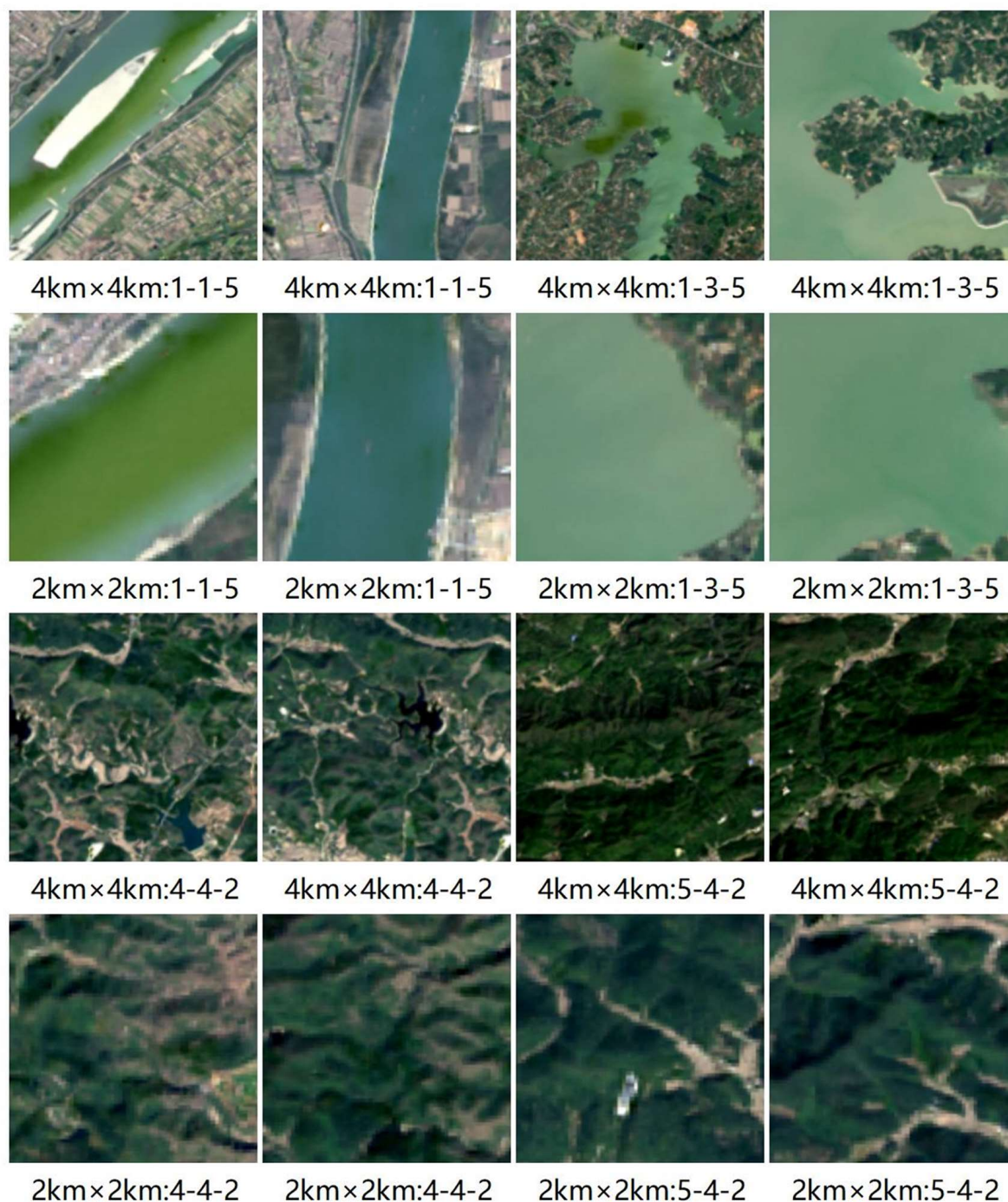
Figure 9. Same landscape character at different research scales.

4.3. Future Directions for Landscape Character Analysis

The AI landscape character classification system, the AI-LC classifier, results in an approximately 10% misclassification rate. The process of classification learning and category optimization allows for understanding the reasons behind the similarities among landscape characters, thereby revealing the impact of both natural and social elements on the landscape character.

At the macro-scale, there is high similarity between Grade 1 and 2 farmland landscapes. The characteristic features of plain farmland represent the core landscape of the Jianghan Plain hinterland. However, the landscape of transition areas differs from that of plain farmland landscapes, with stepped farmland created by changes in terrain and the complex

environment of farmland intermingled with water bodies, resulting in a distinct landscape character. With respect to the forest landscape, woodlands in the north and southeast exhibit distinct characters at the macro-scale, which are influenced by their respective surrounding environments. This differentiation diminishes as the research unit area is reduced.

Consequently, choosing appropriate research scales for different regions becomes crucial for future research. With respect to water bodies, the analysis of water areas is particularly important in the Jianghan Plain. This encompasses the study of river landscapes. River landscapes, characterized by their longitudinal continuity, do not align with the standard unit-based approach to water research employed in this study. This aspect warrants further consideration in subsequent research.

As the research scope becomes more refined, the need for enhanced accuracy in primary data grows, especially when a patch contains many landscape characters. This research is confined to macro- and meso-scales. Scales with specific thresholds are established. The determination of these thresholds aids in defining the scope of content pertinent to each research scale. However, when these thresholds are set, certain combined types emerge because the location is a composite of multiple landscape characters, thus constituting distinctive landscape characters. Characteristic landscapes are more likely to emerge in typical areas and at the intersections of large plateaus.

There is a need to enhance the interpretation of images that have yet to be correctly recognized further, for example, in complex landscapes composed of farmland, water areas, and forest land. While the identification results may indicate that this landscape cannot be accurately identified, its intricate features nonetheless contribute to its status as a region with distinct landscape characters. This kind of landscape may become more prevalent with an increase in the study scale and less so as the scale decreases.

5. Conclusions

Existing research on landscape character assessment mostly focused on small-scale targets such as urban streetscapes and agricultural landscapes; few applications were directed toward the classification of complex landscape characteristics within diverse and intricate environments, like the Jianghan Plain. This research created a set of landscape character categories and an associated remote sensing image dataset based on LANMAP for the Jianghan Plain, then proposed a landscape character recognition model named the AI-LC classifier to identify various landscape characters at multiple scales with deep neural networks. The AI-LC classifier delineated 10 macro- and 18 meso-landscape characters with a precision of 89% and 86%, respectively, demonstrating its effectiveness for the automatic analyses of landscape characters for large and complex regions. Inspired by the results of macro-level analyses, the Jianghan Plain was segmented into four major zones, namely the lake network river basin, the hillfront terrace, the surrounding mountains, and the lake network island hill, offering further insights for landscape planning and conservation.

In future research, we can further refine the integration of the AI-LC classifier with various landscape environmental indicators, enhance its ability to classify and interpret high-precision remote sensing data, and thus achieve the classification and research of landscape character types at a more detailed microscopic scale. To further develop the potential of artificial intelligence in environmental science, this classifier is a beneficial tool for landscape character planning and management in China and advancing global landscape management strategies.

Author Contributions: W.Q.: writing—original draft, methodology, investigation, conceptualization. W.L.: data curation, software, visualization. Z.Z.: investigation, conceptualization, validation. W.C.: writing—review and editing, visualization, methodology, funding acquisition. M.W.: project administration, methodology, supervision, funding acquisition. All authors have read and agreed to the published version of the manuscript.

References

1. Mücher, C.A.; Klijn, J.A.; Wascher, D.M.; Schaminée, J.H.J. A New European Landscape Classification (LANMAP): A Transparent, Flexible and User-Oriented Methodology to Distinguish Landscapes. *Ecol. Indic.* **2010**, *10*, 87–103. [CrossRef]
2. McAlpine, G. *Landscape Character Assessment—Guidance for England and Scotland*; The Countryside Agency: London, UK, 2002.
3. Diechuan, Y.; Chi, G. Analysis of Five Topics in Multi-Scale Identification of Landscape character in Europe. *Landsc. Archit.* **2024**, *31*, 14–22. [CrossRef]
4. Warnock, S.; Griffiths, G. Landscape Characterisation: The Living Landscapes Approach in the UK. *Landsc. Res.* **2015**, *40*, 261–278. [CrossRef]
5. Antrop, M.; Van Eetvelde, V. *Landscape Perspectives*; Landscape Series; Springer: Dordrecht, The Netherlands, 2017; Volume 23, ISBN 978-94-024-1181-2.
6. Van Eetvelde, V.; Antrop, M. A Stepwise Multi-Scaled Landscape Typology and Characterisation for Trans-Regional Integration, Applied on the Federal State of Belgium. *Landsc. Urban Plan.* **2009**, *91*, 160–170. [CrossRef]
7. Yang, D.; Gao, C.; Li, L.; Van Eetvelde, V. Multi-Scaled Identification of Landscape Character Types and Areas in Lushan National Park and Its Fringes, China. *Landsc. Urban Plan.* **2020**, *201*, 103844. [CrossRef]
8. Güngöroğlu, C.; Kavgacı, A.; Coşgun, U.; Çalıkoğlu, M.; Örtel, E.; Balpınar, N. Applicability of European Landscape Typology in Turkey (Çakırlar Watershed Case/Antalya). *Landsc. Res.* **2018**, *43*, 831–845. [CrossRef]
9. Wang, Y.; Du, J.; Kuang, J.; Chen, C.; Li, M.; Wang, J. Two-Scaled Identification of Landscape Character Types and Areas: A Case Study of the Yunnan–Vietnam Railway (Yunnan Section), China. *Sustainability* **2023**, *15*, 6173. [CrossRef]
10. Pan, Y.; Wu, Y.; Xu, X.; Zhang, B.; Li, W. Identifying Terrestrial Landscape Character Types in China. *Land* **2022**, *11*, 1014. [CrossRef]
11. Li, G.; Zhang, B. Identification of Landscape Character Types for Trans-Regional Integration in the Wuling Mountain Multi-Ethnic Area of Southwest China. *Landsc. Urban Plan.* **2017**, *162*, 25–35. [CrossRef]
12. Wu, Z.; Lu, Q.; Lei, S.; Yan, Q. Study on Landscape Ecological Classification and Landscape Types Evolution: A Case Study of a Mining City in Semi-Arid Steppe. *Sustainability* **2021**, *13*, 9541. [CrossRef]
13. Carlier, J.; Doyle, M.; Finn, J.A.; Ó hUallacháin, D.; Moran, J. A Landscape Classification Map of Ireland and Its Potential Use in National Land Use Monitoring. *J. Environ. Manag.* **2021**, *289*, 112498. [CrossRef] [PubMed]
14. Larrachea, I.U.; Poggio, S.L.; Cosentino, D.; Semmartin, M. The Hidden Heterogeneity of Agricultural Landscapes of the Rolling Pampa (Argentina). *Agric. Ecosyst. Environ.* **2022**, *332*, 107934. [CrossRef]
15. Li, H.; Zhang, C.; Zhang, S.; Ding, X.; Atkinson, P.M. Iterative Deep Learning (IDL) for agricultural landscape classification using fine spatial resolution remotely sensed imagery. *Int. J. Appl. Earth Obs. Geoinf.* **2021**, *102*, 102437. [CrossRef]
16. Fang, Z.; Lu, W.; Zhu, F.; Zhu, C.; Li, Z.; Pan, J. Landscape Classification System Based on RKM Clustering for Soil Survey UAV Images–Case Study of the Small Hilly Areas in Jurong City. *Sensors* **2022**, *22*, 9895. [CrossRef] [PubMed]
17. Giang, T.L.; Bui, Q.T.; Nguyen, T.D.L.; Dang, V.B.; Truong, Q.H.; Phan, T.T.; Nguyen, H.; Ngo, V.L.; Tran, V.T.; Yasir, M.; et al. Coastal Landscape Classification Using Convolutional Neural Network and Remote Sensing Data in Vietnam. *J. Environ. Manag.* **2023**, *335*, 117537. [CrossRef]
18. Guo, M.; Liu, H.; Xu, Y.; Huang, Y. Building Extraction Based on U-Net with an Attention Block and Multiple Losses. *Remote Sens.* **2020**, *12*, 1400. [CrossRef]
19. Chen, Y.; Ming, D.; Lv, X. Superpixel Based Land Cover Classification of VHR Satellite Image Combining Multi-Scale CNN and Scale Parameter Estimation. *Earth Sci. Inform.* **2019**, *12*, 341–363. [CrossRef]
20. Wang, H.; Chen, X.; Zhang, T.; Xu, Z.; Li, J. CCTNet: Coupled CNN and Transformer Network for Crop Segmentation of Remote Sensing Images. *Remote Sens.* **2022**, *14*, 1956. [CrossRef]
21. Wei, M.; Wang, H.; Zhang, Y.; Li, Q.; Du, X.; Shi, G.; Ren, Y. Investigating the Potential of Sentinel-2 MSI in Early Crop Identification in Northeast China. *Remote Sens.* **2022**, *14*, 1928. [CrossRef]
22. Xiong, Y.; Zhang, Q.; Chen, X.; Bao, A.; Zhang, J.; Wang, Y. Large Scale Agricultural Plastic Mulch Detecting and Monitoring with Multi-Source Remote Sensing Data: A Case Study in Xinjiang, China. *Remote Sens.* **2019**, *11*, 2088. [CrossRef]
23. Chen, D.; Ma, A.; Zheng, Z.; Zhong, Y. Large-Scale Agricultural Greenhouse Extraction for Remote Sensing Imagery Based on Layout Attention Network: A Case Study of China. *ISPRS J. Photogramm. Remote Sens.* **2023**, *200*, 73–88. [CrossRef]
24. Zhang, W.; Tang, P.; Zhao, L. Fast and Accurate Land-Cover Classification on Medium-Resolution Remote-Sensing Images Using Segmentation Models. *Int. J. Remote Sens.* **2021**, *42*, 3277–3301. [CrossRef]
25. Zhang, L.; Wang, L.; Wu, J.; Li, P.; Dong, J.; Wang, T. Decoding Urban Green Spaces: Deep Learning and Google Street View Measure Greening Structures. *Urban For. Urban Green.* **2023**, *87*, 128028. [CrossRef]
26. Wu, Y.; Liu, Q.; Hang, T.; Yang, Y.; Wang, Y.; Cao, L. Integrating Restorative Perception into Urban Street Planning: A Framework Using Street View Images, Deep Learning, and Space Syntax. *Cities* **2024**, *147*, 104791. [CrossRef]

27. Sun, H.; Xu, H.; He, H.; Wei, Q.; Yan, Y.; Chen, Z.; Li, X.; Zheng, J.; Li, T. A Spatial Analysis of Urban Streets under Deep Learning Based on Street View Imagery: Quantifying Perceptual and Elemental Perceptual Relationships. *Sustainability* **2023**, *15*, 14798. [CrossRef]

28. Meng, L.; Wen, K.-H.; Zeng, Z.; Brewin, R.; Fan, X.; Wu, Q. The Impact of Street Space Perception Factors on Elderly Health in High-Density Cities in Macau—Analysis Based on Street View Images and Deep Learning Technology. *Sustainability* **2020**, *12*, 1799. [CrossRef]

29. Zhang, L.; Pei, T.; Wang, X.; Wu, M.; Song, C.; Guo, S.; Chen, Y. Quantifying the Urban Visual Perception of Chinese Traditional-Style Building with Street View Images. *Appl. Sci.* **2020**, *10*, 5963. [CrossRef]

30. Zhang, J.; Fukuda, T.; Yabuki, N. Development of a City-Scale Approach for Façade Color Measurement with Building Functional Classification Using Deep Learning and Street View Images. *ISPRS Int. J. Geo-Inf.* **2021**, *10*, 551. [CrossRef]

31. Li, Y.; Yabuki, N.; Fukuda, T. Integrating GIS, Deep Learning, and Environmental Sensors for Multicriteria Evaluation of Urban Street Walkability. *Landsc. Urban Plan.* **2023**, *230*, 104603. [CrossRef]

32. Liu, J.; Gu, W.; Liu, Y.; Zhang, C.; Li, W.; Shao, D. Dynamic Characteristics of Net Anthropogenic Phosphorus Input and Legacy Phosphorus Reserves under High Human Activity—A Case Study in the Jianghan Plain. *Sci. Total Environ.* **2022**, *836*, 155287. [CrossRef]

33. Wan, M.; Liu, M.; Huang, J.; Liu, F. The Research and Analysis of Ecological Wisdom in Urban Eight Scenes—Taking Jianghan Plain as an Example. *Chin. Landsc. Archit.* **2022**, *38*, 18–25. [CrossRef]

34. Yang, X.; Zhou, X.; Shang, G.; Zhang, A. An Evaluation on Farmland Ecological Service in Jianghan Plain, China—From Farmers' Heterogeneous Preference Perspective. *Ecol. Indic.* **2022**, *136*, 108665. [CrossRef]

35. Geng, B.; Tian, Y.; Zhang, L.; Chen, B. Evolution and Its Driving Forces of Rural Settlements along the Roadsides in the Northeast of Jianghan Plain, China. *Land Use Policy* **2023**, *129*, 106658. [CrossRef]

36. He, K.; Zhang, X.; Ren, S.; Sun, J. Deep Residual Learning for Image Recognition. In Proceedings of the IEEE Conference on Computer Vision and Pattern Recognition, Las Vegas, NV, USA, 27–30 June 2016; pp. 770–778.

37. Li, Z.; Liu, F.; Yang, W.; Peng, S.; Zhou, J. A Survey of Convolutional Neural Networks: Analysis, Applications, and Prospects. *IEEE Trans. Neural Netw. Learn. Syst.* **2022**, *33*, 6999–7019. [CrossRef]

38. Comber, A.; Fisher, P.; Brunsdon, C.; Khmag, A. Spatial Analysis of Remote Sensing Image Classification Accuracy. *Remote Sens. Environ.* **2012**, *127*, 237–246. [CrossRef]

39. Yang, R.; Li, X.; Mao, D.; Wang, Z.; Cheng, L.; Dong, Y.; Sun, H. A Methodological Framework for Prioritizing Wetland Restoration from Cropland: A Case Study Jianghan Plain, China. *Land Use Policy* **2024**, *137*, 107025. [CrossRef]

40. Gan, Y.; Wang, Y.; Duan, Y.; Deng, Y.; Guo, X.; Ding, X. Hydrogeochemistry and Arsenic Contamination of Groundwater in the Jianghan Plain, Central China. *J. Geochem. Explor.* **2014**, *138*, 81–93. [CrossRef]

41. Shu, L.; Li, X.; Chang, Y.; Meng, X.; Chen, H.; Qi, Y.; Wang, H.; Li, Z.; Lyu, S. Advancing Understanding of Lake–Watershed Hydrology: A Fully Coupled Numerical Model Illustrated by Qinghai Lake. *Hydrol. Earth Syst. Sci.* **2024**, *28*, 1477–1491. [CrossRef]